PHYSICAL REVIEW B VOLUME 18, NUMBER 12 15 DECEMBER 1978

Short-pulse optical studies of exciton relaxation and F-center formation in NaCl, KCl, and NaBr

R. T. Williams, J. N. Bradford, and W. L. Faust
Naval Research Laboratory, Washington, D. C. 20375
(Received 11 July 1978)

Using short-pulse laser techniques, the formation time and absolute production efficiency of F centers in KCl have been investigated on the time scale of 10^{-11} sec. The temperature-dependent yield of F centers observable at 46 psec following two-photon band-gap excitation has been determined over the range 12–880 K in crystalline KCl. The yield of F centers per ionizing event approaches unity near the melting point. The observation of transient 532-nm absorption resulting from ultraviolet pulse irradiation of molten KCl is reported. The formation time, production efficiency, and room-temperature decay time of self-trapped excitons in the lowest triplet state in NaCl have been investigated, as has the onset of 532-nm absorption in NaBr. The observations, in general, place upper limits of a few picoseconds on the time for capture of an electron by a hole in these alkali halides when carrier densities are in the range of 5×10^{17} cm^{-3}. Recently proposed mechanisms of F-center formation are discussed in light of the present results. We develop mathematically convenient treatments for convolution of pulse shapes and intrinsic photochemical response in several kinetic models.

I. INTRODUCTION

Recombination of electrons and holes in defect-free parts of alkali-halide crystals generally proceeds through a sequence of intermediate states involving local rearrangement of the lattice ions. For example, holes self-trap spontaneously in alkali halides, becoming localized in molecular orbitals formed principally from the valence shells of two adjacent halide ions which are thereby bonded in a relaxed lattice configuration.[1] The excited states resulting from capture of an electron by a self-trapped hole, i.e., self-trapped excitons (STE), give rise to most of the intrinsic recombination luminescence in alkali halides.[2,3] Relaxation of free electrons and holes to the luminescent STE states involves several processes describable by characteristic times. It is generally assumed that hole self-trapping occurs in times of the order of 10^{-13}–10^{-12} sec. Self-trapping of a low-energy exciton may take substantially longer than this at low temperature.[4] No direct measure of these relaxation times has yet been attempted, though a measurement could in principle be made by monitoring the characteristic uv-absorption band of the self-trapped hole or the corresponding transition of the self-trapped exciton (STE). Self-trapped holes capture conduction electrons within a time which depends on carrier concentration. One important result of the work presently being reported is the establishment of an upper limit (10 psec) on the time for electron capture by self-trapped holes at carrier densities in the range 10^{17}–10^{18} cm^{-3}.

An electron bound in a high Rydberg state about the self-trapped hole must relax across large energy gaps separating the lowest STE states (e.g., 2 eV in NaCl) before reaching the luminescent triplet state, $^3\Sigma_u^+$.[5] For this reason, relaxation to $^3\Sigma_u^+$ might be expected to require a time as long as 10^{-8} sec. We have investigated the time for relaxation to the lowest STE triplet state in NaCl at 15 and 295 K by monitoring the onset of absorptive transitions out of $^3\Sigma_u^+$ after electron-hole generation. The subnanosecond decay of this state to the ground state at 295 K has also been observed, and the yield of electron-hole pairs reaching $^3\Sigma_u^+$ has been measured. The population of $^3\Sigma_u^+$ in NaCl at low temperature apparently occurs much faster than the corresponding process observed in KI by Suzuki and Hirai.[6]

Self-trapped excitons are also central to the photochemical damage process of vacancy-interstitial pair production in halides, and provide channels for rapid nonradiative recombination across the band gap (typically 6–12 eV). Formation of unstable F-H pairs represents in some cases the dominant relaxation channel. The F center is a halide-ion vacancy trapping one electron and the H center is the complementary interstitial halogen atom. A close F-H pair is apparently unstable against restoration of the crystal ground state on a time scale of microseconds or much less.[7] Defects that achieve larger separations may be stable, particularly at low temperature.

Time-resolved optical measurements are particularly useful in identifying reaction routes, in determining formation times, and in measuring the formation yield of inherently unstable products. Using short-pulse laser techniques, we have investigated F-center production on the

 © 1978 The American Physical Society

scale of 10^{-11} sec. An initial study of the F-center formation time in KCl using these techniques has been described in an earlier Letter.[8] We have repeated those measurements with refinements in the apparatus and have performed additional experiments to place limits on the sample temperature during irradiation and on the role of preexisting defects. The short-pulse techniques have been used to make measurements of the absolute efficiency of formation of primary defects, defined as those observable 46 psec after initial excitation of the crystal, at temperatures from 12 to 880 K in crystal KCl. We have performed exploratory experiments to observe optical absorption resulting from ultra-violet excitation of molten KCl, presumably due to photochemically produced "defects" in the liquid.

NaBr was chosen for study as a material whose F band is accessible to our 532-nm probe pulse, and that differs from KCl in having an F-production efficiency that is very small at low temperature and increases with temperature in anti-correlation with the intrinsic luminescence. In both NaBr and NaCl there is evidence of a component of absorption which is produced very rapidly and decays in less than the 25-psec duration of the probe pulse. A similar rapidly decaying component of absorption has been reported for KI by Suzuki and Hirai.[6] Possible explanations for such short-lived absorption include very close F-H pairs and "hot" self-trapped excitons.

Beyond our immediate interest in exciton relaxation and production of lattice defects in alkali halides, the experimental techniques of photophysics developed or extended in this work should be generally applicable to many materials.

II. ABSORPTION RISE TIME

A. Experiment

In these experiments, a passively mode-locked, pulsed YAlG:Nd laser oscillator provided trains of 1.06-μm pulses in the TEM_{00} mode. Single pulses with energies of 0.5 – 1.0 mJ were selected by a Pockels cell operated from a laser-triggered spark gap. The mean pulse duration was 30 psec with an extreme fluctuation range of about ±5 psec, as determined in previous streak-camera and two-photon-fluorescence measurements. The pulses had approximately a symmetrical Gaussian shape. An amplifier provided gain up to 25 for those experiments requiring more than the oscillator energy. The second harmonic (532 nm) was generated in deuterated potassium dihydrogen phosphate (d-KDP) with efficiency ranging from about 40% without the amplifier to about 60% with 20× amplification. For the measurements of defect-formation time, the fourth harmonic was produced in 90° phase-matched ammonium dihydrogen phosphate (ADP) with a limiting efficiency of about 8% relative to the 1.064-μm fundamental.

Since our earlier Letter,[8] we have modified the apparatus used for the study of F-center formation time to allow for a simpler and more accurate determination of relative delay between excitation and probe pulses. In the present arrangement (Fig. 1), the combined green and uv pulses, coincident except for group-velocity dispersion in the fourth-harmonic generator, pass under mirror M_3 and are incident on a 45° fused-silica prism (P) oriented for minimum deviation. After reflection from a translatable reflector (M_1), the dispersed uv pulse (U) returns to the prism, elevated so as to emerge slightly above the incident beam. Similarly, the green pulse G_2 partially reflected by mirror M_2 emerges from P collinearly with U. Hairline marks on the prism are used for accurate alignment. Pulses U and G_2, now above the plane of the incident beam, are reflected by mirror M_3 toward the sample as excitation and probe pulses. Since mirrors M_1 and M_2 are located side by side with edges about 1 mm apart, their relative displacements can be directly compared within ±10 μm by the use of a machinist's microscope. Then from detailed consideration of the optical-path geometry and group-velocity dispersion, the relative mirror positions for pulse coincidence can be established. The smallest uncertainty in pulse coincidence attainable with the techniques of sighting and align-

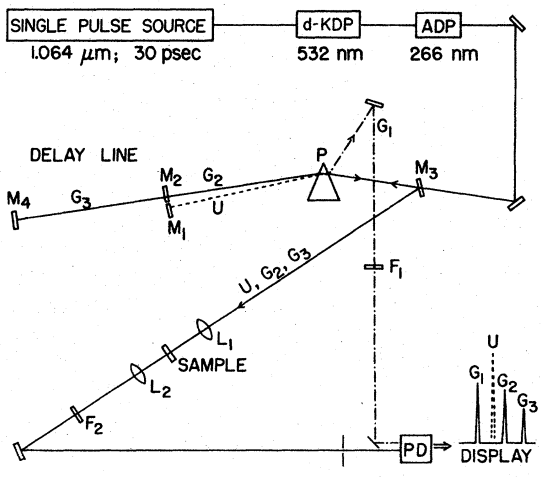

FIG. 1. Apparatus for measurement on a picosecond time scale of absorption at 532 nm following two-photon excitation by a 266-nm pulse. Pulses G_1, G_2, G_3, and U are reference, early probe, late probe, and ultraviolet excitation pulses, respectively.

ment developed over the course of this investigation is estimated to be ±1 psec. For most of the data presented here, the uncertainty in determining pulse coincidence is ±3 psec. Uncertainties in the absorption data and in the curve-fitting procedure are comparable or larger.

Green light transmitted by the partial mirror M_2 is returned collinearly with G_2 by a *pair* of mirrors (M_4) arranged in the vertical plane. This pulse (G_3) serves to assess absorption several nanoseconds after excitation. In the present work G_3 follows G_2 by 7 nsec. An intensity reference for normalization (G_1) is developed by directing the green pulse reflected from the first surface of the prism to the photo-diode (PD) along a path a few nanoseconds shorter than that of the probe pulse. Green and uv pulses are focused into the sample by a fused silica lens (L_1) as in the previous work. The green probe pulse comes to a focus near the first surface of the sample and is centered on a larger defocused uv spot. The green focal spot on the crystal is imaged onto the photo-diode or for setup, onto a viewing screen with a magnification of about 70. Three pulses appear on the oscilloscope screen in time sequence. U (not part of the display) can be shifted in time relative to G_1, G_2, and G_3.

The high-purity single-crystal KCl used in these experiments was grown at the Naval Research Laboratory by the Bridgman method, under an atmosphere of argon saturated with carbon tetrachloride. This treatment has been shown to remove virtually all anionic contamination and all cations except the alkali and alkaline-earth metals. Hydroxyl-ion contamination is approximately 0.2×10^{-6} OH^- per Cl^-. Pieces measuring typically $14\times14\times1$ mm^3 were cut from the central region of the crystal and polished. (Some samples with cleaved surfaces were also used in experiments, with no evident difference in results.) The bulk absorption coefficient of this crystal at 10.6 μm was measured calorimetrically to be 10^{-4} cm^{-1}. This is only about 25% above the intrinsic multiphonon absorption level and attests to the high purity of the material.[9] The NaCl and NaBr crystals used in this work were grown at Harshaw Chemical Co. and Naval Research Laboratory, respectively.

For low-temperature experiments, the sample was mounted in a cold-finger cryostat. LiF and CaF_2 windows in the cryostat were used for the production-yield experiments. In all the experiments the uv beam was well out of focus when passing through the windows, and no significant nonlinear or transient absorption effects were found even in SiO_2 windows. The energy density of absorbed uv, typically 0.5 J/cm^3, produces no significant heating of the sample at temperatures of 78 K and higher. If all of the absorbed ultraviolet light were to be dissipated immediately as heat, the irradiated spot in a KCl crystal initially at liquid-helium temperature should reach about 23 K. Since a significant fraction of the absorbed energy is radiated as luminescence or stored in the form of lattice defects and trapped charges, the actual temperature rise should be less. To provide an experimental test of the uv-pulse-induced temperature rise at nominal liquid-helium temperature, we have measured the decay time of luminescence from the lowest triplet state of self-trapped excitons created in KCl by the uv pulse, under the same typical pulse-power conditions used for the F-center absorption experiments. The KCl luminescence is known to decay with a time constant of 5 msec at temperatures below 12 K.[10] The time constant drops by about two orders of magnitude between 12 and 20 K.[11] Under the test conditions, we measured the luminescence decay time to be 5.0 msec, with no evidence of multiple decay components that would arise from nonuniform heating of some areas above 12 K. Thus we conclude that the local temperature after uv-pulse irradiation in the experiments on KCl was no higher than 12 K when liquid helium was the coolant. This is in fact a lower temperature than would be expected if luminescence and F-center formation were the only channels competing with heat production.

B. Data analysis

Let G_1, G_2, and G_3 denote transmitted pulse energies when no ultraviolet pulse is allowed to strike the sample. Let G_1', G_2', and G_3' be the transmitted energies when the sample is excited by an ultraviolet pulse which is advanced a time Δ relative to pulse G_2. Then the effective optical density for probe delay Δ is

$$D(\Delta)=\log_{10}(G_1'G_2/G_1G_2'). \tag{1}$$

The optical density after a fixed delay of 7 nsec is a similar expression involving $G_1'G_3$ and G_1G_3'. The experimental data are displayed as the ratio $D(\Delta)/D(7\text{ nsec})$, typically normalized to unity at the maximum relative density attained, $D_{max}/D(7\text{ nsec})$. Error bars represent $\pm\sigma N^{-1/2}$, where σ is the standard deviation of N data points at a given probe pulse delay.

If the optical absorption rises on the time scale of the laser-pulse duration, analysis of the onset of absorption requires treatment of convolution integrals (see the Appendix). The green-probe-pulse intensity $G(t)$ is taken to be a normalized Gaussian function whose typical full width at half

maximum (FWHM) is 25 psec. The rate of two-photon carrier generation in the sample should then be approximately a Gaussian function $C(t)$ whose width is between 0.5 and roughly 1 times the width of G, depending on pulse depletion and group-velocity mismatch in the redoubling crystal. With $F(t,\Delta)$ representing the fraction of the maximum density D_{max} which has developed by time t, we write an expression for $D(\Delta)$:

$$D(\Delta) = -\log_{10}\int_{-\infty}^{\infty} dt\, G(t)\exp[-aF(t,\Delta)], \tag{2}$$

where

$$F(t,\Delta) = \int_{-\infty}^{t} dt'\, K(t-t')C(t'+\Delta). \tag{3}$$

$G(t)$ and $C(t)$ are both normalized to unit area, and $a = 2.303D_{max}$. $K(t-t')$ describes the intrinsic coloration process. For the material studies presented here, it is not necessary to introduce coherent coupling between the excitation and probe pulses (see the Appendix and discussion of NaBr).

In Fig. 2 we plot several members of the family of curves parametrized by D_{max}, assuming that population of the absorbing level is instantaneous, i.e., taking $K(t-t')$ to be unity. Figure 2(a) corresponds to the case in which both the excitation of carriers and the probe pulse have equal widths, $W_C = W_G$. Figure 2(b) represents the case $W_C = 0.5W_G$. Calculations for square pulses and triangular pulses have yielded results very similar to those for the Gaussian pulses in Fig. 2. For symmetrical pulses in general, $D(0)/D_{max}$ is independent of pulse width as long as W_C and W_G scale together. For useful working values of D_{max}, the fraction $D(0)/D_{max}$ is almost independent of the relative widths of excitation and probe pulses and has a value near 0.4.

A small delay in the physical process of populating the absorbing level can be most simply represented in this model by taking $K(t-t'-\delta)$ to be a step function which is zero for negative argument and unity otherwise. The effect is to translate the curves in Fig. 2 by δ. Then by noting the value of Δ for which $D(\Delta)/D_{max} \approx 0.4$, one can make a quick estimate of the physical delay time.

Another tractable model assumes exponential growth of absorbing centers:

$$K(t-t') = 1 - \exp[-(t-t')/\tau]. \tag{4}$$

The time constant τ then serves as at least an approximate characterization of the speed of production of the absorbing species. In the Appendix, Eqs. (2)–(4) are developed in a form that can be conveniently used in curve fitting.

If the population of absorbing centers decays exponentially with the time constant τ_2, then the function

$$K(t-t') = \frac{\tau_2}{\tau_2-\tau_1}\exp\left(-\frac{(t-t')}{\tau_2}\right) \times\left\{1-\exp\left[-(t-t')\left(\frac{1}{\tau_1}-\frac{1}{\tau_2}\right)\right]\right\} \tag{5}$$

is to be used in Eq. (3). (D_{max} may then be redefined depending on the values of τ_1 and τ_2.) Equation (5) comes from considering a simple three-level system governed by first-order kinetics, in which the upper level decays to the middle level with time constant τ_1, and the middle level decays to the lowest level with time constant τ_2. The middle level could represent F centers, for example, with the first and third

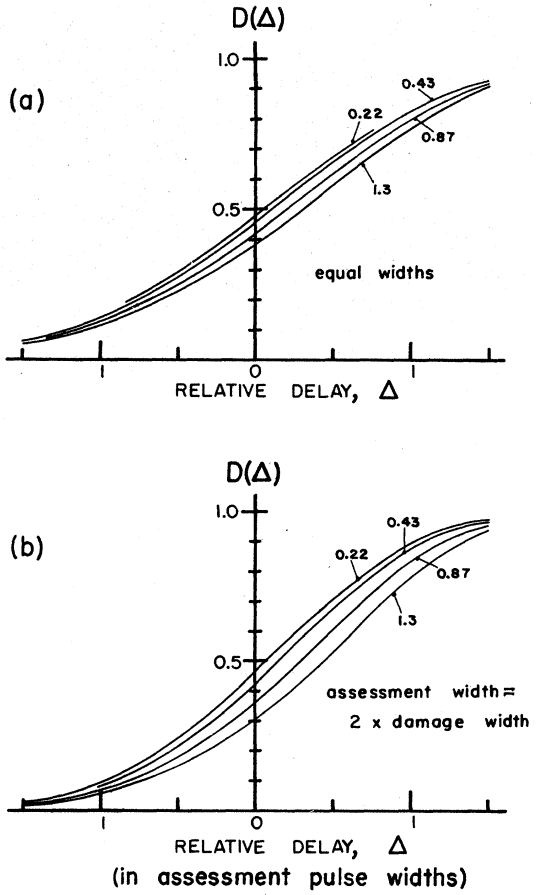

FIG. 2. Family of curves representing Eq. (2) under the assumption of an instantaneous process of coloration, $K(t-t')=1$, is plotted for several values of the parameter $a = 2.303D_{max}$. In (a) the excitation and probe pulses are of equal width, while in (b) the excitation pulse is half the duration of the probe pulse.

levels representing the F precursor and crystal ground state. Applying Eq. (5) to the data of Suzuki and Hirai[6] for KI at liquid-He temperature yields $\tau_1 \approx 12$ psec and $\tau_2 \approx 15$ psec. This and the more general problem of serial decay are discussed in the Appendix.

In fitting our present data, we have in some cases hypothesized that the observed absorption is the sum of a stable component and a separate unstable component. In principle, we would then take K to be a sum of terms proportional to Eqs. (4) and (5). In some cases the formation and decay times of the unstable component have typically been shorter than the laser pulse, and there is not enough detail in the data to extract both time constants reliably. As a simplification in such cases, we assume that the unstable component is formed instantaneously, and write

$$K(t-t') = C_1(1 - e^{-(t-t')/\tau}) + C_2 e^{-(t-t')/\tau_2}. \quad (6)$$

C. F centers in KCl

Figure 3 shows the rise of 532-nm absorption in KCl at $T \approx 12$ K after two-photon generation of electron-hole pairs. Since 532 nm is very near the peak of the F band at low temperature, and in view of spectral measurements at 85 psec reported earlier,[8] we can be reasonably confident that the rise of absorption in Fig. 3 corresponds to the production of F centers. These data are essentially a repeat of previously published results for KCl.[8] The difference is that with the apparatus of Fig. 1, zero delay can be determined more precisely than before, and by means of the experiment on luminescence quenching, the temperature of the irradiated spot is known more accurately. Fitting the data to Eqs. (2) and (4) with $W_C = W_G = 25$ psec and $D_{max} = 0.5$ yields the rise time $\tau = 9$ psec. The estimated uncertainty is ±5 psec. A rise time $\tau = 11 \pm 9$ psec in KCl was found in Ref. 8.

Fitting the data with a single exponential component clearly involves some assumptions. However aside from a small dip occurring just after the maximum absorption is attained, there is no indication that the more complicated expressions, Eqs. (5) or (6), are needed. The absorption decays to about 80% of its maximum value in 7 nsec at 12 K.

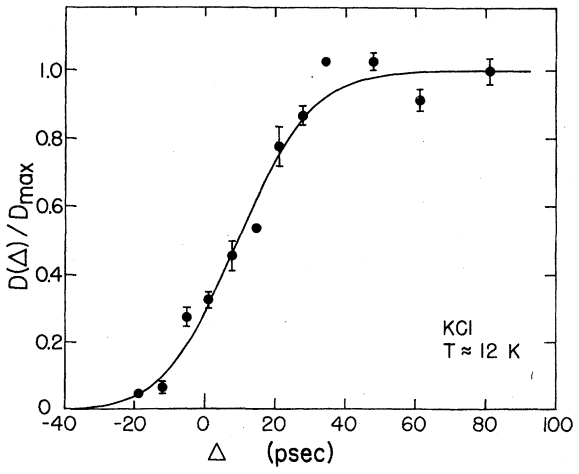

FIG. 3. For KCl at $T \approx 12$ K, we plot fractional optical density $D(\Delta)/D_{max}$ after the 266-nm excitation pulse. The curve is a best-fit convolution of pulse shapes with an exponential form for defect production [Eqs. (2) and (4)], yielding $\tau \approx 9$ psec. Error bars denote $\pm\sigma N^{-1/2}$, where σ is the standard deviation of N measurements at a given delay.

D. Self-trapped excitons in NaCl

On the right-hand side of Fig. 4 is shown the transient absorption spectrum of metastable triplet self-trapped excitons in NaCl, as mea-

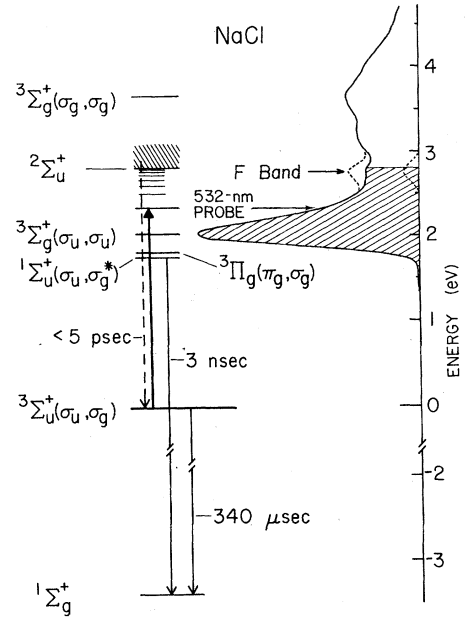

FIG. 4. Energy levels of the self-trapped exciton in NaCl are shown along with the transient absorption spectrum as measured a few microseconds after electron pulse excitation at 10 K (Ref. 5). The transient absorption spectrum also includes the F band shown by the dashed curve. The heavy arrow originating in $^3\Sigma_u^+$ corresponds to absorption of a 532-nm probe photon in the present experiment. The dashed arrow is a schematic representation of the population of $^3\Sigma_u^+$ from free-carrier states, observed in this experiment to occur in less than 5 psec. The 3-nsec fluorescence and 340-μsec phosphorescence transitions are also indicated.

sured following electron pulse excitation at low temperature.[5] Energy levels are represented on the left-hand side of the figure. The initial state for both the intrinsic 367-nm luminescence and the observed transient absorption is $^3\Sigma_u^+(\sigma_u, \sigma_g)$ where the hole occupies a $3p$ σ_u orbital localized on the relaxed chloride-ion pair and the electron occupies a rather extended σ_g orbital about the Cl_2^- core. At temperatures below 50 K, the lifetime of $^3\Sigma_u^+$ is 340 μsec. The low-energy absorption peak and its shoulder (shown shaded) have been attributed to Rydberg-like excitations of the electron bound to the self-trapped hole.[5] The series limit ($^2\Sigma_u^+$) is approximately 2.8 eV. According to available data, there is an energy gap of about 1.8 eV between $^3\Sigma_u^+$ and the next-higher state at the equilibrium relaxation coordinate for the STE.[12] Therefore if $^3\Sigma_u^+$ is populated directly from $^3\Sigma_g^+(\sigma_u, \sigma_u)$ across a 1.8-eV energy gap, one might expect a substantial delay in population of $^3\Sigma_u^+$. In the present experiment, two-photon absorption of the 266-nm laser pulse creates free electrons and holes. The experiment measures the onset of absorption corresponding to transitions from $^3\Sigma_u^+$ to states lying just above $^3\Sigma_g^+(\sigma_u, \sigma_u)$. The rise time of absorption is thus a measure of the time of relaxation from free electrons and holes to $^3\Sigma_u^+$. The results for low temperature ($T \approx 15$ K) are shown in Fig. 5(a). The dashed line is a convolution of Gaussian excitation and probe pulses according to Eqs. (2) and (3), assuming instantaneous relaxation to a stable absorbing state. (Parameters are $W_C = W_G = 25$ psec and $D_{max} = 0.65$.) The experimental onset of absorption *precedes* this model curve by a margin which is outside the experimental

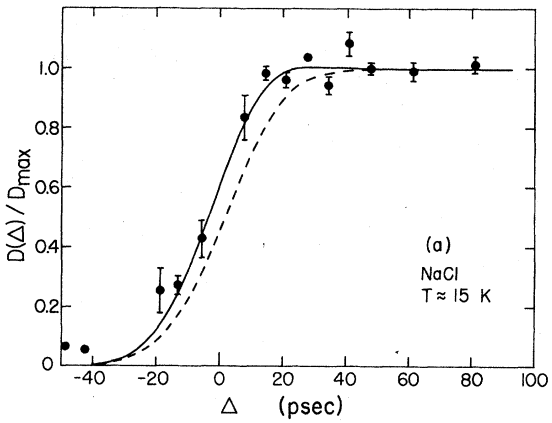

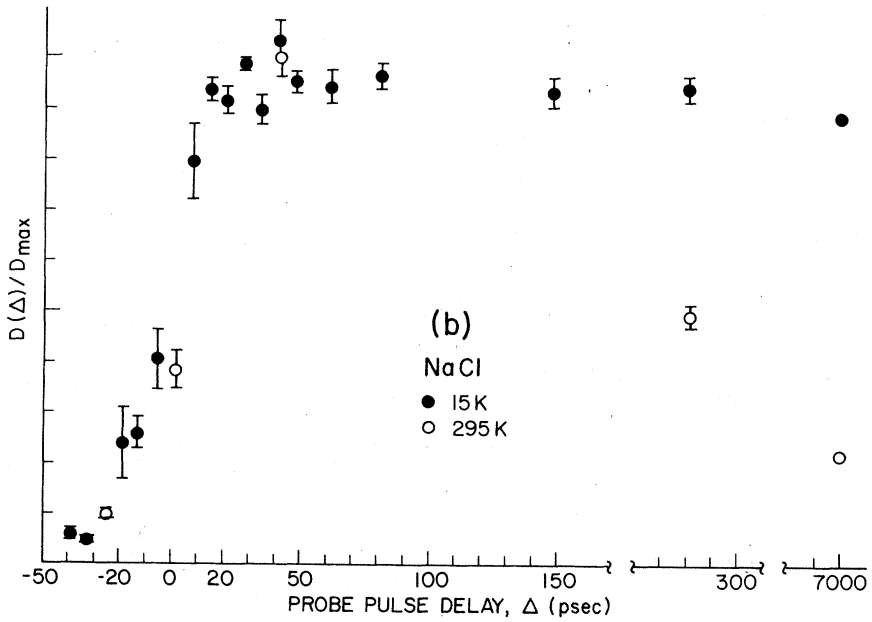

FIG. 5. (a) For NaCl at $T \approx 15$ K, we plot fractional optical density $D(\Delta)/D_{max}$ at 532 nm vs delay (Δ) after the 266-nm excitation pulse. The dashed curve is a convolution of pulse shapes assuming instantaneous formation of stable defects. The solid curve is a best-fit convolution of pulse shapes with two components of absorption [Eq. (7)]. Both components are assumed to be formed instantaneously. One remains stable on this time scale, and the other decays in about 2.5 psec. (b) Fractional optical density at 532 nm in NaCl at 295 and 15 K is shown for longer times after excitation.

error in determination of pulse coincidence. A better fit is obtained with Eqs. (2) and (6), including a second component of absorption that decays rapidly. The resulting time constants are $\tau \approx 0$ for the rise of absorption that remains stable during the interval shown, and $\tau_2 \approx 3$ psec for the decay of the second component. In using Eq. (6), the second component is assumed to rise instantaneously. Other parameters are $C_2/C_1 = 2.5$ and $W_C = W_G = 25$ psec. Because of the number of parameters involved, the time constants and ratio C_2/C_1 are known only approximately.

The long-lived component of absorption is effectively linked with the spectral measurements made by electron-pulse excitation.[5] The rapidly decaying component of absorption has some precedent in the observations on KI by Suzuki and Hirai.[6] They ascribed a short-lived component to very close or "incomplete" F-H pairs. This is a possible explanation for our observation in NaCl, since the absorption due to close F-H pairs can be expected to lie between the normal F band and the low-energy STE band. That is, our 532-nm probe might be very close to the peak of such a perturbed F-center transition. Inspection of Fig. 4 reveals another possible origin of the short-lived absorption in NaCl. Our probe samples the steep edge of the 2-eV band and should therefore register an increase of absorption if the band is thermally broadened, where all else remains the same. Since the lowest STE triplet state lies about 3 eV below the initial 9.32-eV excitation energy of the e-h pair, relaxation to that state will be accompanied by substantial vibrational excitation of local lattice modes. It is thus possible that we are observing vibrational cooling of the newly created STE triplet during the 25-psec laser pulse. Spectral measurements with better than 10-psec resolution would provide more certain identification.

It is especially interesting that the time required for free electrons and holes to relax to the lowest STE state $^3\Sigma_u^+$ is so different in KI and NaCl. Suzuki and Hirai found the relaxation process to take 210 psec in KI at liquid-He temperature,[6] whereas it takes less than 5 psec in NaCl at 15 K. Data on the thermal quenching of the lowest STE triplet state in the temperature range 11 to 100 K have been found to fit an equation relating the observed lifetime τ to the radiative lifetime τ_R and thermally activated nonradiative decay[13]:

$$1/\tau = 1/\tau_R + \nu e^{-E/kT}.$$

For NaCl,

$$\tau_R = 3.4 \times 10^{-4} \text{ sec},$$
$$\nu = 4.1 \times 10^{10} \text{ sec}^{-1}, \quad (7)$$
$$E = 0.099 \text{ eV}.$$

The present data afford an opportunity to test the applicability of this formula to self-trapped excitons at a temperature where the luminescence is fully quenched. The value of τ at 295 K predicted by Eq. (7) is 1.2 nsec. Relying primarily on the point at 280 psec, the present data are consistent with $\tau \approx 0.38$ nsec. The absorption persisting at 7 nsec is probably due to the F band, which partially overlaps the 532-nm probe wavelength at room temperature.

1. NaBr

Our initial interest in making measurements of absorption rise times in NaBr was provoked by the contrast between the temperature dependence of stable defect yield in NaBr and KCl. The efficiency of formation of stable F centers in NaBr is very low at temperatures below about 150 K and then increases in anticorrelation with the self-trapped exciton (STE) luminescence.[14] In KCl F centers are formed with rather high efficiency even at 4 K, and anticorrelation with STE luminescence is not apparent. The possibility that a different, possibly slower, defect-formation mechanism is at work in NaBr led to our measurements of the rise of 532-nm absorption, since the F-band peak in NaBr is about 540 nm at low temperature.

The measurements in NaBr at 295 K are shown in Fig. 6. The curve is a pulse convolution in-

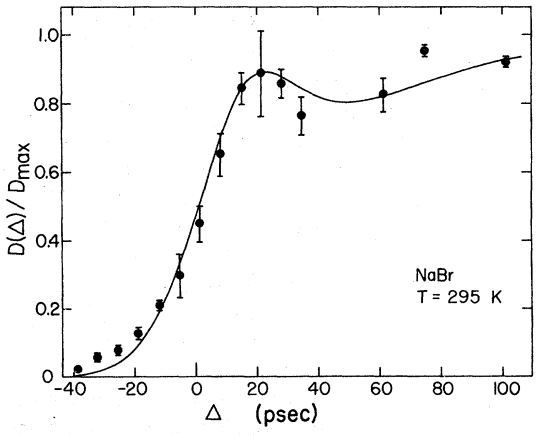

FIG. 6. For NaBr at $T = 295$ K, we plot fractional optical density at 532 nm vs delay (Δ) after the 266-nm excitation pulse. The curve is computed from Eqs. (2), (4), and (5), assuming that a stable absorption component grows with exponential time constant $\tau = 38$ psec, and that an unstable component grows with $\tau_1 = 10$ psec and decays with $\tau_2 = 5$ psec.

cluding a stable component of absorption described by Eq. (4) with $\tau \approx 38$ psec, and an unstable component described by Eq. (5) with $\tau_1 \approx 10$ psec, and $\tau_2 \approx 5$ psec. Possibilities for the origin of the absorption include unstable F centers or short-lived states of self-trapped excitons. Detailed spectral measurements will be required to sort out the possibilities. Thus a new temporal component of absorption induced in NaBr by e-h pair generation has been found, but these rise-time measurements have not yet adequately answered our initial question about the rate of F-center production in NaBr.

The 1s exciton peak in NaBr at $T = 10$ K is at 6.71 eV,[15] compared with the energy (7.02 eV) corresponding to the sum of a 266-nm photon and a 532-nm photon. Thus we must consider the possibility that the 532-nm probe light might be absorbed by a two-photon process involving the 266-nm pulse when the uv and green pulses overlap in the sample. Frohlich and Staginnus[16] have shown that in KBr, which also has the low-temperature 1s exciton peak at 6.71 eV, the two-photon absorption threshold is 7.26 eV at 20 K and about 7.10 eV at 80 K. By analogy, two-photon absorption of 266- and 532-nm photons in NaBr is marginally possible. However, two-photon absorption would only be evident in Fig. 6 as a peak centered at $\Delta = 0$, and cannot contribute to the absorption which is observed at times longer than about 20 psec after pulse coincidence.

III. PRIMARY-DEFECT PRODUCTION EFFICIENCY

An attempt to measure the absolute yield of lattice defect formation in halide crystals necessitates a definition of the time scale on which the defects are recognized as existing. One may, for example, restrict attention to those defects which are observable on time scales accessible to most traditional measurement techniques, i.e., times longer than a few seconds. It is this definition of the defect problem which relates in a practical sense to material properties in steady state. Stabilization of the defects is then a major factor determining the production efficiency.

The term "primary defects" has been used to designate the more inclusive category of all vacancy-interstitial pairs formed initially, i.e., including those which are ultimately annihilated or altered as the stable population is established. It is expected that photochemical processes or relaxation dynamics, rather than stabilization of the reaction products, will be the main factors in primary-defect production. As Sonder has pointed out, however, even this more inclusive category is subject to the definition, related closely to measurement technique, of what constitutes the initial defects.[17] In recent measurements of formation efficiency based on annihilation of aggregate centers by interstitials, he considered that the primary F-H pair production efficiency relates to F centers and H centers which achieve sufficient separation that they move more or less independently of one another.[17] In time-resolved spectroscopy utilizing electron pulse excitation the primary defects have been considered to be those observable on a nanosecond time scale. It is probably not true that the same population is being studied in both cases. In addition, there might be other defects recombining in subnanosecond times, especially at high temperatures. Using techniques of picosecond optical spectroscopy, we have undertaken in the present work to extend the temporal limits on the measurement of primary-defect production yield to the range of 10^{-11} sec.

A. Experiment

The measurement of defect production yield requires a determination of the uv energy density deposited in the crystal and of the resulting defect population. To make that possible, the test region must be uniformly irradiated by the uv, and the relatively small probe spot must be centered within the uv spot. Fourth-harmonic generation for the experiments on defect production yield was accomplished using deuterated KDP, which afforded conversion efficiency of about 17% relative to 532 nm and better beam quality than with temperature-tuned ADP. Spatial examination of the beams with a silicon-diode array indicated that the second-harmonic beam profile was nearly Gaussian and that the fourth-harmonic beam generated in deuterated KDP was approximately Gaussian with a low-frequency, low-contrast, noiselike modulation. For the formation-time measurements, spatial modulation in the uv pulse is of less concern. However, the production-yield experiment demands a uniform distribution.

In the apparatus that fulfills these requirements (Fig. 7), pulses G_2 and U are centered on a 600-μm pinhole in their path to the sample. Assuming a Gaussian intensity distribution across the probe beam, the pinhole aperture is uniformly illuminated within about 5%. The spatial modulation on the uv beam was fairly reproducible, and it was possible to choose a region of the uv beam in which there was little structure within the pinhole aperture. The diode array indicates a deviation from uniformity of less than 10%, adequately satisfying the experimental require-

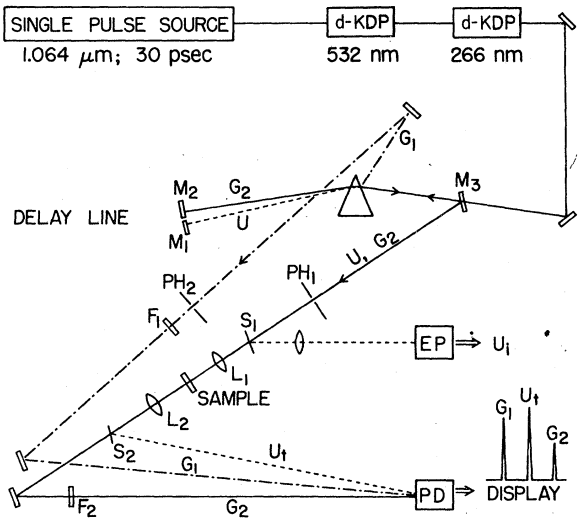

FIG. 7. Apparatus for measurement on a picosecond time scale of the production efficiency of photoinduced defects or excited states. The incident (U_i) and transmitted (U_t) 266-nm excitation pulses, as well as the reference (G_1) and probe (G_2) 532-nm pulses are recorded by means of a pyroelectric energy probe (EP) and calibrated photodiode (PD). A circular spot of known size and nearly uniform ultraviolet illumination is obtained by imaging a 600-μm pinhole (PH_1) on the surface of a thin sample.

ment. Observation of two-photon-induced F-center coloration during alignment also proved a useful guide in attaining conditions for uniform illumination.

Lens L_1 forms an ultraviolet image of the pinhole on the front face of the sample. Since the pinhole diffracts light, care must be taken that the image on the sample is of the pinhole and not of a strongly ringed diffraction pattern that appears beyond the pinhole. Microscopic examination confirmed that the probe beam was adequately centered within the uv-irradiated spot. To provide a gauge of absolute energy, a fused-silica beamsplitter (S_1) reflects part of the uv pulse through an imaging lens to a pyroelectric energy probe (EP). After correction for reflectance of S_1 and reflection losses in lenses and windows, this yields the uv energy incident on the sample (U_i). The ultraviolet light transmitted by the sample (U_t) is partially reflected by beam splitter S_2 to the photodiode (PD). With no sample in place, the photodiode is calibrated to give absolute uv energy, and the difference between the incident and transmitted energies, corrected for reflection at the sample surfaces, is the uv energy absorbed by the crystal.

The samples we have dealt with are all thin, of the order of 1 mm or less. With the pinhole imaged on the sample, the uv beam is conical and well defined throughout the sample thickness. For a 1-mm crystal, the cross-sectional area of the beam increases from front to back by about 15%.

B. F centers in KCl

Using the experimental arrangement of Fig. 7, with the 532-nm probe pulse following the 266-nm excitation pulse by 46 psec, the two-quantum ultraviolet energy deposition and the resulting 532-nm absorption in KCl were measured as a function of temperature between nominal liquid-helium temperature and 880 K. With the known temperature dependence of the F- band width and peak position as detailed below, these measurements yield the efficiency for production of primary F centers—i.e., that fraction of electron-hole pairs excited with 9.32 eV energy which yield F centers observable 46 psec later (Fig. 8).

In relating the measured optical density to the number of F centers produced, we have used the Smakula equation for a Gaussian band. The experimental conditions assure that the coloration density is nearly uniform in any plane perpendicular to the propagation direction of the probe beam. The distribution along the propagation direction is not uniform, but the Smakula equation can be readily written in a form relating the optical density to the number of centers encountered per unit cross-sectional area sampled by the probe beam, regardless of the longitudinal

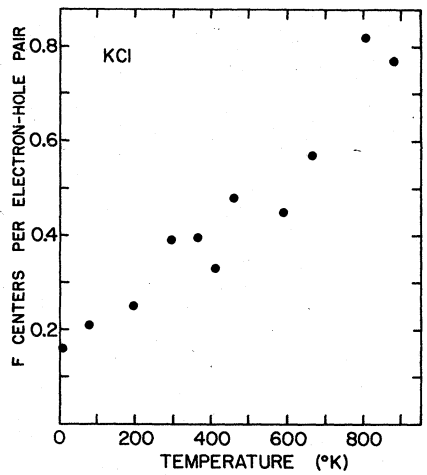

FIG. 8. From measurements of 532-nm absorption made 46 psec after band-gap excitation of KCl by a 266-nm pulse, the number of F centers produced per two-photon absorption event has been computed. The production efficiency has been corrected for the temperature dependence of the F-band spectrum and approximately for a small component of 532-nm absorption due to self-trapped excitons.

distribution:

$$\frac{F \text{ centers}}{\text{cm}^2} = 2.0 \times 10^{17} \frac{n}{(n^2+2)^2} \frac{W}{f} D_m, \quad (8)$$

where D_m is the optical density at the peak of the band, W is the FWHM in eV, and n is the refractive index. For the F band in KCl, and for the Lorentz effective field used in the Smakula equation, we take the oscillator strength to be $f = 0.58$. This is the average of four determinations listed in a recent review by Smith and Dexter.[18] The refractive index at 530 nm in KCl is 1.494 at 293 K, and is corrected approximately for temperature by taking $dn/dt = -3.6 \times 10^{-5}$ (K^{-1}) to apply at all temperatures.[19]

The F-band width in eV as a function of temperature in KCl can be written[20]

$$W = 0.163[\coth(71.0/T)]^{1/2} \quad (9)$$

and the peak position shifts with temperature according to

$$E_m = 2.340 - 0.027 \coth(71.0/T). \quad (10)$$

At low temperature, our probe wavelength of 532 nm (2.33 eV) is very near the peak of the F band. At higher temperatures the peak shifts to longer wavelengths, but because of simultaneous broadening of the absorption, the 532-nm probe wavelength falls well within the F band even at 880 K. For the point at 12 K in Fig. 4, we have taken the F-band width to be 0.22 eV as suggested by the 85-psec spectrum in Ref. 8. This is intermediate between the stable F-band width at 12 K of 0.163 eV and the perturbed width of 0.30 eV found by Hirai *et al.*[21]

In the present experiment, we measure the total absorption at 532 nm, which includes a small contribution from self-trapped excitons in addition to F centers. From the data of Ref. 5 it is seen that STE bands constitute about 12% of the total absorption at 532 nm as measured 1 μsec after excitation at 10 K. We have reported low-temperature spectral data in KCl measured about 85 psec after F-band formation, using three additional probe wavelengths derived from 532 nm by stimulated Raman scattering in benzene.[8] The data are consistent with STE absorption roughly 10% of the F-band peak, but no more than 25%. The correction to be made for STE absorption at higher temperature is less certain, because the corresponding spectral data do not yet exist. We assume that the branching ratio of electron-hole pairs to the lowest triplet STE state does not increase with temperature above 12 K in KCl. This is consistent with luminescence data. Then the correction for STE absorption is approximated in Fig. 8 by subtracting 0.02, the low-temperature STE contribution, from all yields. With almost 80% of all electron-hole pairs yielding an F center at 880 K, and 16% even at temperatures as low as 12 K, the production of defects is clearly a major channel for relaxation of electronic excitation in KCl. From measurements of luminescence efficiency, Purdy *et al.* have found that about 10% of electron-hole pairs created in KCl at low temperature yield intrinsic luminescence from the self-trapped exciton.[22] Thus F-center production competes favorably with population of the lowest relaxed exciton levels, and at high temperature it competes favorably with all other processes combined.

Another aspect of Fig. 8 to be noted at this stage of the discussion is that the defect yield is apparently a monotonically increasing function of temperature. This behavior is in contrast to the complicated temperature dependence of the stable F-center yield measured in steady state, as summarized by Sibley and Sonder.[23] Figure 9 displays the ratio of the F-center yield measured 10 sec after band-gap excitation to the 46-psec yield given in Fig. 8. The 10-sec yields were measured with the same apparatus (Fig. 7) used for measurement of yields at 46 psec. The following pulse sequence was employed: A 266-nm pulse generated electron-hole pairs by two-photon absorption, and a 532-nm pulse trailing by 46 psec effected a measurement of the early F-center absorption as detailed above. The crystal then remained in darkness for 10 sec, whereupon another single 532-nm probe pulse was used to measure the residual absorption. By repeating the measurement with one probe pulse incident each second of the delay period, it was determined that bleaching of the F centers by one probe pulse is not significant.

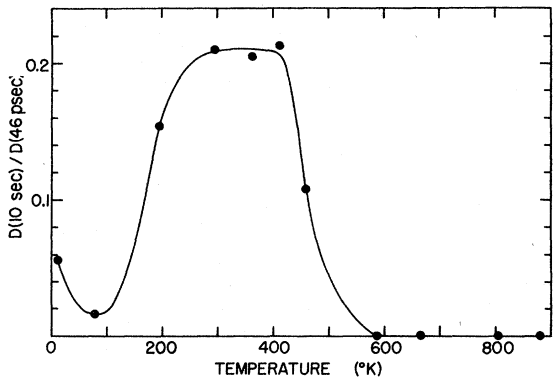

FIG. 9. Ratio of optical densities at 532 nm measured 10 sec and 46 psec after band-gap excitation of KCl is plotted as a function of crystal temperature.

In the temperature range up to 300 K, the general agreement between published yields of stable F-center production and the 10-sec yields in Fig. 9 is quite good. The main difference is that the stable F-center yield reaches a maximum near 200 K and then falls off gradually toward 300 K, whereas the 10-sec yield increases up to 300 K and starts to decrease only above 400 K. This difference indicates that the F-band absorption at room temperature continues to decrease on a time scale of 10 sec or more after formation, up to times of the order of minutes when most conventional measurements of defect yield would be made. Also, we have observed that at room temperature the F band in KCl decreases by about 35% in the first 5 nsec after formation. Thus it can be expected that the F-center yield measured at 10 or 20 nsec after excitation (e.g., by electron pulse) will display some of the character of Fig. 9 as a function of temperature, since some annealing of close defect pairs occurs within the measurement time.

A question crucial to the interpretation of all the data being presented is whether the F centers we observe by this technique are in fact new lattice defects created by the ultraviolet laser pulse, or whether bare anion vacancies (α centers) already existing in the crystal are populated with conduction electrons generated by the uv pulse. In a previous Letter[8] we presented arguments, based largely on the F-center relaxation time of 0.6 μsec, that electron capture at a vacancy should not affect low-temperature measurements on a subnanosecond time scale. Our ability in the present work to measure absolute defect yields affords an opportunity to address the above question in a more quantitative fashion. Thus, the defect yield in a virgin area of the KCl crystal was compared to the yield (both at 46 psec and 10 sec) in an area of the crystal which had been heavily colored by multiple exposures to the uv laser pulse and then bleached by exposure to white light. This treatment should result in a sample containing a large concentration of negative-ion vacancies. Figure 9 indicates that in the virgin KCl crystal at 12 K, the F-center concentration remaining at 10 sec is only 6% of the concentration at 46 psec. However when that same spot or another spot on the crystal had been treated to introduce a high concentration of bare vacancies, the coloration observable at 46 psec was less than in the virgin crystal for the same uv energy absorbed and the coloration subsequently increased by a factor of up to 2.7 as measured at 10 sec.

The increasing coloration between early and late times in a crystal containing prior radiation damage has previously been demonstrated for pulsed electron irradiation of KCl.[24] The phenomenon was explained in terms of the long relaxation time of an electron captured at a vacancy. In the present work we have demonstrated that the same argument holds under the conditions of laser-pulse experiments. The lower 46-psec yield in the vacancy-containing area of the crystal probably is partly a result of vacancies and F centers competing with holes for available electrons, thereby reducing the e-h recombination events available to initiate production of new F-H pairs. Linear absorption of the 266-nm pulse by damage products absorbing in the uv, thereby depleting the uv energy available to make e-h pairs, may also have an effect. The substantial decrease of F-center concentration between 46 psec and 10 sec in the virgin crystal has already been discussed in terms of annihilation of close F-H pairs. Thus in summary we can say that the signature of newly created F-H pairs at low temperature is a decrease of the early (46 psec) absorption to $\lesssim$6% at 10 sec, while the signature of F centers formed by electron capture at vacancies is an absorption increasing to as much as 2.7 times the initial value. These measurements indicate that in our virgin KCl samples the typical photogenerated F-H pair concentration exceeded the concentration of native vacancies capable of single-pulse conversion to F centers by a factor of at least 40. This conclusion should preclude electron-trapping at vacancies from having any substantial effect on the present measurements in KCl.

A natural extension of our studies of the high-temperature yield of defects in KCl crystals was to carry the study above the melting point. The results are of interest in relation to questions of polaron effects and temporary short-range order in an ionic liquid, and may indicate a sort of point-ion analog of the solvated electron problem, which has been treated extensively in the literature.[25] To perform the experiments we ground up a pure single crystal of KCl and loaded the powder into a clean, dry fused-silica cell having a 1-mm optical path length. This cell was placed in an oven in the laser optical path and heated (in air) to melt the KCl. Using the same techniques as for solid samples, the liquid KCl was excited by a 266-nm pulse and then probed 46 psec later with a 532-nm pulse. Transient absorption of 532-nm light resulting from the 266-nm pulse was distinctly observed. Since we do not presently know the shape or width of the absorption band, the data cannot be analyzed in terms of concentration. Instead, we simply state that using the same geometry and spot size as for the solid-

KCl measurements, an absorbed uv energy density of 0.2 J/cm^2 resulted in optical density at 532 nm of 0.17. For comparison, 0.74 optical density for 0.05 J/cm^2 absorbed energy represents the corresponding efficiency in solid KCl at 880 K, where the absolute F-center yield per e-h pair is about 0.8. An absorption band in molten KCl is likely to be very broad, so our observations can be quite consistent with a high yield of absorbing states.

In this regard, we note the recent observation by Clark of an optical-absorption band in molten KBr held in equilibrium with excess potassium vapor.[26] At 1028 K, the band has a FWHM of 1.42 eV and its peak is at about 1.20 eV, estimated from data taken above 1.1 eV. For comparison, the F band in solid KBr at 870 K has a width of 0.65 eV and its peak is about 1.75 eV.[27]

At the uv power densities employed for the experiments in liquid KCl, the transmittance of 266-nm light through 1 mm of solid KCl would be roughly 50% at all submelting temperatures. We found that the 266-nm pulses were almost totally absorbed in a 1-mm path of liquid KCl a few degrees above the melting temperature. This change of absorptivity was reversible with subsequent freezing or melting. The onset of uv transmittance seemed to be prompt upon freezing, but the transmitted light persisted (though fading) for about 10 sec after melting. Strong absorption of 266-nm light in liquid KCl is consistent with the observations of Clark, Skull, and Wells on broadening of the fundamental absorption edge in molten alkali halides.[28] They found that the absorption edge in liquid KCl can be described by the empirical Urbach rule,

$$\alpha(E) = \alpha_0 \exp[-\sigma(E_0 - E)/kT],$$

where $E_0 = 6.22$ eV and $\sigma = 0.63$.

C. Self-trapped excitons in NaCl

The efficiency of populating the STE state $^3\Sigma_u^+(\sigma_u, \sigma_g)$ in NaCl at 15 K, i.e., STE yield per e-h pair created at 9.32 eV, was measured by essentially the same techniques used for F centers in KCl. In NaCl the 532-nm probe samples the major low-energy STE peak at a point where the absorption is 40% of the maximum, as indicated in Fig. 4. The probe does not sample the unperturbed F band in NaCl at low temperature. To relate optical density at the probe wavelength to a number S of self-trapped excitons per irradiated area of the sample, we use the Smakula equation in a form similar to Eq. (8), but not assuming a Gaussian band:

$$S = 8.21 \times 10^{16} \frac{n}{(n^2+2)^2} f^{-1} \int D(E)\, dE. \qquad (11)$$

The optical density $D(E)$ was scaled to its measured value at the probe photon energy. Then using the STE spectrum in Fig. 4, $D(E)$ was integrated over the spectral range (shaded in Fig. 4) corresponding to the Rydberg series of the STE. An oscillator strength (f) of unity was assumed for the integrated Rydberg series. We have used the Lorentz effective field, with the refractive index 1.556. Dividing S by twice the number of uv photons absorbed per unit area of the sample, we find that the yield of self-trapped excitons in the $^3\Sigma_u^+$ state is 0.19 per 9.32-eV excitation at a temperature $T \approx 15$ K.

IV. DISCUSSION

A. Electron capture

In the present experiments, free electrons and holes are created by absorption of two ultraviolet photons totaling 9.32 eV. We observe that the carriers experience mutual capture into states at least 2 eV below the conduction-band edge (e.g., F-H pairs or self-trapped excitons) in less than 10 psec. From the measurements of defect production efficiency and from the absence of a slow component in the formation of F centers or self-trapped excitons, we can infer that essentially all of the initially free carriers must recombine or be trapped within 10 psec under the present experimental conditions. This rapid recombination is observed throughout the temperature range from 12 K to the melting point of KCl.

Because of the strong electron-phonon coupling in alkali-halide crystals, the carriers thermalize very rapidly. It is generally assumed that holes self-trap very quickly, e.g., 10^{-13}–10^{-12} sec. However, it is not immediately obvious that recombination or deep trapping of the electrons should occur in less than 10^{-11} sec in these experiments. For example, measurements of photoconductivity in KBr and KI excited by two-photon absorption across the band gap have shown that for carrier concentrations below 10^{12} cm^{-3} the carrier lifetime against recombination or deep trapping is of order 10^{-8} sec.[29] A carrier lifetime of 1 μsec under similar conditions in KI has been reported.[30]

Conditions in the present experiment differ from those of photoconductivity measurements in two main regards. No electric field is applied in the present work, and the carrier densities are much higher, typically 5×10^{17} cm^{-3}. The lifetimes determined from photoconductivity were approximately independent of applied electric

field in the range 10^3–10^4 V/cm employed in the experiments. Furthermore, such fields are smaller than the Coulomb field within a 100-Å radius of a unit electron charge imbedded in a medium of dielectric constant 6. Therefore it is unlikely that the applied electric fields used in photoconductivity could reduce the deep trapping rate by three to five orders of magnitude as observed.

On the other hand, it can be expected that the carrier recombination rate should increase with carrier concentration. Band-to-band Auger transitions have been shown to cause rapid recombination at high carrier densities in a number of semiconductors.[31] In this three-body process, an electron-electron collision in the presence of a hole results in nonradiative electron-hole recombination, with the third particle gaining kinetic energy equivalent to the recombination energy. However, such band-to-band recombination would compete with the lattice defect formation or exciton self-trapping which we observe, rather than contributing to it. Since the Auger recombination rate increases as the third power of carrier concentration, one would predict on that basis that an increase in the concentration of excited carriers should cause only a very limited increase in the yield of F centers or self-trapped excitons if Auger recombination is important. This was specifically not observed in our present measurements. The defect yield was found to be proportional to the photogenerated carrier concentration. Therefore we conclude that band-to-band Auger recombination is not an important channel at carrier concentrations of order 5×10^{17} cm^{-3} in the alkali halides being studied.

Instead, we suggest that the recombination at fairly high carrier densities is governed by second-order kinetics. In a simple model for bimolecular decay, the time-dependent carrier concentration $n(t)$ is related to the initial concentration n_0 by

$$n(t)=n_0(1+t/\tau)^{-1}, \quad \tau=(v\sigma n_0)^{-1}, \tag{12}$$

where τ is the time for n to fall to $\frac{1}{2}$ its initial value, v is an average electron velocity (the holes are self-trapped), and σ is the cross section for electron capture by a self-trapped hole to yield defects, self-trapped excitons, or band-to-band recombination. Since the half life in bimolecular decay is inversely proportional to the initial concentration, carrier lifetimes of 10^{-8} sec observed for $n_0=10^{12}$ cm^{-3} could scale into the picosecond range for $n_0=5\times10^{17}$ cm^{-3}. If the present experiments were done with initial carrier concentrations smaller by one or two orders of magnitude, the measured defect formation times might show effects of the slower carrier recombination.

Since the total impurity or defect concentration in most halide crystals is at least 10^{17} cm^{-3}, it is striking that capture of electrons at self-trapped holes so dominates other trapping processes when the carrier concentration is of the order of 5×10^{17} cm^{-3}. Evidently self-trapped holes have very large electron-capture cross sections. Assuming that the electron-capture process accounts for the entire 9-psec F-center formation time in KCl and that bimolecular kinetics apply, we can estimate a lower limit on the cross section for electron capture by a self-trapped hole. A reasonable estimate of the velocity of a photoexcited electron corresponds to one optical-phonon energy, since cooling to about $\hbar\omega_{LO}$ above the band edge proceeds very rapidly by LO-phonon emission, and thereafter by slower emission of acoustical phonons. In that case, $v\approx10^7$ cm/sec and Eq. (12) yields $\sigma\gtrsim2\times10^{-14}$ cm^2.

B. Exciton relaxation

It will be helpful in the course of further discussion to refer to the qualitative configuration-coordinate diagram for the exciton-defect system shown in Fig. 10. The left-hand side of the dia-

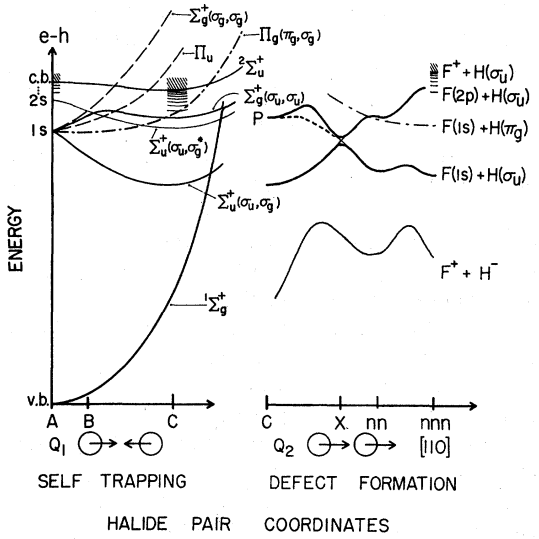

FIG. 10. Qualitative potential-energy curves representing two intersecting planes in the multidimensional configuration-coordinate space for electron-hole pairs in alkali halides are shown, including free excitons at A, self-trapped excitons at C, and F–H defect pairs at nearest-neighbor (nn) and next-nearest-neighbor (nnn) separations. Two coordinates of a halide-ion pair are represented. The stretching mode (Q_1) is largely responsible for self-trapping. Generalized translation of the halide pair (Q_2) begins the defect-formation process.

gram refers to exciton self-trapping. The coordinate represented is the symmetric stretching mode (along ⟨110⟩) of a pair of nearest-neighbor halide ions. Corresponding diagrams for specific alkali-halide crystals have been discussed in some detail.[5,32] Coordinate value A corresponds to the perfect lattice. The zero of energy is taken at the valence-band (VB) edge, from which excitations to free-exciton states (labeled $1s, 2s, \ldots$) or conduction-band (CB) states may occur. In all of the present experiments, two-photon absorption of 266-nm light creates a free electron and hole (e-h) near lattice coordinate A. Subsequent relaxation of the e-h pair may populate one of the metastable radiative states of the self-trapped exciton at coordinate value C, i.e., ${}^3\Sigma_u^+(\sigma_u, \sigma_g)$ or ${}^1\Sigma_g^+(\sigma_u, \sigma_g^*)$. Ultimately the electronic ground state of the crystal is restored by radiative or nonradiative transitions. Although the band gap is from 6 to 12 eV in the alkali halides, nonradiative transitions across the band gap can occur with high probability. The dominant mechanism is crossover to the ground state in the relaxed lattice, ${}^1\Sigma_g^+$, which intersects the excited states for Q_1 coordinate values rather near C.

The energy levels represented in Fig. 4 for NaCl correspond to the Q_1 coordinate value C in Fig. 10. The energy gap separating $\Sigma_u^+(\sigma_u, \sigma_g)$ and states near $\Sigma_u^+(\sigma_u, \sigma_g^*)$ at C is almost 2 eV, and yet the relaxation to ${}^3\Sigma_u^+(\sigma_u, \sigma_g)$ takes less than 5 psec. In retrospect that is not so surprising since three different paths for rapid relaxation can be identified in Fig. 10. ${}^1\Sigma_g^+$ cuts across all the states, as does an entire Rydberg sequence of states built on a π_g rather than a σ_u hole. The lowest such state, $\Pi_g(\pi_g, \sigma_g)$ is shown by the chain curve. In addition, relaxation to the F-H defect state in the right half of Fig. 10 has been shown to be rapid and highly probable in KCl.[8] Attempts at defect formation which fail to achieve a metastable configuration and instantly undergo recombination to populate a lower STE state constitute a likely channel for rapid STE relaxation. Although there are evidently many possible paths for rapid relaxation of higher STE states to ${}^3\Sigma_u^+(\sigma_u, \sigma_g)$ or ${}^1\Sigma_g^+$, it should be noted that there is one higher state, ${}^1\Sigma_u^+(\sigma_u, \sigma_g^*)$, with a lifetime of about 3 nsec. The rapid-relaxation channel is evidently fairly selective.

C. *F*-center formation

Among the recent suggestions of mechanisms for production of vacancy-interstitial pairs in alkali halides,[33-36] there is general concurrence on several basic points. These can be summarized with the aid of the right half of Fig. 10, which represents translation of the halide-ion pair toward an interstitial atom configuration (the H center), leaving behind a vacancy with one trapped electron (the F center). The diagram is to be viewed as a slice through the complete configuration-coordinate space for the e-h pair in an alkali-halide lattice, intersecting the plane corresponding to coordinate Q_1 near point C. The coordinate Q_2 is represented schematically as translation of two ions along the line joining their centers. The true motion is likely to be more complicated, possibly involving rotation of the ion pair in moving toward the nearest-neighbor interstitial position.[37] The subsequent motion comprising a halogen-atom replacement sequence has been discussed elsewhere.[38,39]

Present models and experiment agree that defect production is not initiated from the radiative STE states in most, if not all, alkali halides. The lowest state capable of initiating defect production in KCl has an energy near $\Sigma_g^+(\sigma_u, \sigma_u)$. Since the final defect state $F(1s)+H(\sigma_u)$ correlates adiabatically with $\Sigma_u^+(\sigma_u, \sigma_g)$ the defect precursor (marked P in Fig. 10) at or near $\Sigma_g^+(\sigma_u, \sigma_u)$ is necessarily on a different adiabatic potential surface than is the defect.[37] In principle, the attempted crossing can constitute a bottleneck, limiting the rate of defect formation. The crossover to the lower potential surface is represented at $Q_2 = X$ in Fig. 10.

In a model recently proposed by Toyozawa,[36] the last passage between adiabatic potential surfaces is suggested to occur between STE states in the plane of Q_1, i.e.,

$$\Sigma_g^+(\sigma_u, \sigma_u) \rightarrow \Sigma_u^+(\sigma_u, \sigma_g) .$$

Mixing of these two states by interaction with modes Q_1 and Q_2 was predicted to cause an adiabatic instability of the Q_2 mode. Furthermore it was suggested that a substantial relative shift in the equilibrium value of Q_1 for the two states could allow a nonradiative transition rate large enough to be compatible with the observed F-center formation time of about 10 psec.

Leung and Song have calculated the nonradiative transition rate (W) corresponding to

$$\Sigma_g^+(\sigma_u, \sigma_u) \rightarrow \Sigma_u^+(\sigma_u, \sigma_g)$$

using a molecular-model Hamiltonian expanded in Q_1 and Q_2, and find that W is far too small to be compatible with the observed formation time.[40] By including an additional mode which takes account of the relaxation of other ions around the Cl_2^- molecule, they found a substantially higher nonradiative transition rate. W was computed as a function of a parameter $\Delta\epsilon$, representing the

energy of an optical transition from ${}^3\Sigma_u^+(\sigma_u, \sigma_g)$ to ${}^3\Sigma_g^+(\sigma_u, \sigma_u)$. For $\Delta\epsilon = 1.4$ eV, the nonradiative transition rate W between these two states was calculated to be of the order of 10^{11} sec^{-1} or faster in both NaCl and KCl. However for $\Delta\epsilon = 1.8$ eV, the model calculation predicts $W = 4.8 \times 10^6$ sec^{-1} in NaCl and $W = 1 \times 10^5$ sec^{-1} in KCl.[40] Recent experimental work has now given strong evidence that $\Delta\epsilon = 2.0$ eV in NaCl.[12] This result, in conjunction with earlier observations[5] and trends in recent theoretical calculations for self-trapped excitons in KCl,[41] suggests that $\Delta\epsilon = 1.87$ eV in KCl. Given these parameter values, the calculations of Leung and Song based on a modified formulation of the Toyozawa model predict transition rates generally smaller than indicated by experiment unless a large "strain-energy" parameter describing the symmetric relaxation of ions around the Cl_2^{2-} core is assumed.

Kabler and Williams[37] have discussed qualitatively the probability of nonradiative transitions between the two adiabatic states whose crossing is avoided near X in Fig. 10. Application of the Landau-Zener formula to the states near X shows that for reasonable parameter values, the single-pass crossing probability can be of order unity. In addition it was pointed out that mixing of the ground state of the distorted lattice with the two excited states whose attempted crossing at X is avoided adiabatically can provide alternative fast-relaxation paths.[37] These considerations suggested that the last passage between adiabatic surfaces, if it occurs at X, probably does not constitute a serious bottleneck on the 10-psec time scale.

Yet the defect formation yield is also observed to be temperature dependent, suggesting that barriers are encountered at some point in the relaxation toward metastable defect states. In Fig. 11(a) we plot primary F centers per e-h pair versus reciprocal temperature. The yield does not vary appreciably with reciprocal temperature between 12 and 78 K. In measurements of relative F-center yield following electron-pulse irradiation of KCl from 2 to 78 K, Karasawa and Hirai also found that the yield was approximately constant from 8 to 78 K.[42] Therefore by scaling data in Ref. 42 to match Fig. 11(a) from 12 to 78 K, we obtain the composite curve shown by the solid line in Fig. 11(b). This represents approximately the primary F-center production efficiency from 2 to 880 K. Here the term primary F centers refers to all F centers observable shortly after excitation of the crystal—46 psec for our high-temperature data and a few nanoseconds for the low-temperature data of Karasawa and Hirai. Presumably the observations are early enough to

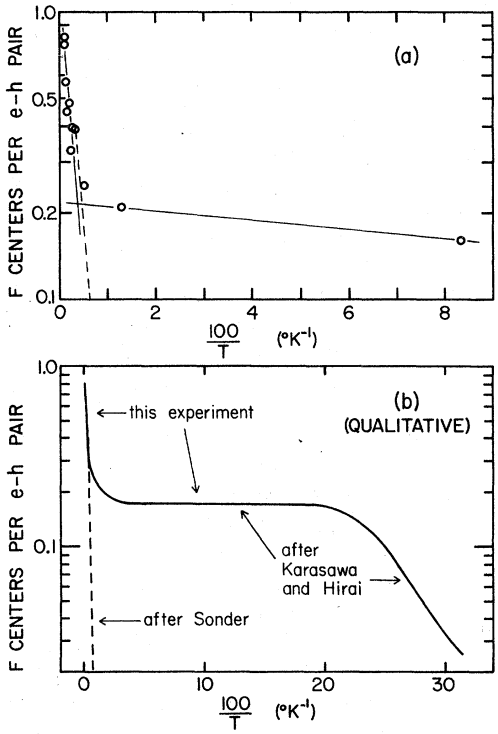

FIG. 11. (a) Defect production efficiency measured in KCl 46 psec after e-h pair generation is plotted vs reciprocal temperature from 12 to 880 K. (b) A composite graph of primary-defect production efficiency in KCl from 2 to 880 K is made by matching the low-temperature data of Karasawa and Hirai (Ref. 42) to the data in (a) at 12 and 78 K. The production efficiency of uncorrelated F and H centers measured by Sonder (Ref. 17) is represented by the dashed line in (a) and (b).

count essentially all defects in KCl before recombination or secondary reactions occur. This would not necessarily be the the case in other materials, however, since very rapidly decaying absorption has been observed in KI,[6] NaCl, and NaBr. Furthermore we will suggest later that there may be very-short-lived defects in KCl which escape detection in the present experiment, but play an essential part in the temperature dependence of defect formation.

The dashed line in Fig. 11 is an approximate representation of the yield of primary F centers in KCl as measured by Sonder using the method of F-aggregate destruction.[17] In this case the primary F-H pairs are defined as those formed "initially" at sufficient separation that subsequent diffusion of the complementary defects is uncorrelated. It is evident from Fig. 11 that the two measurements are not addressing the same defect populations. The short-pulse data count all F centers observable at the time of measurement, including those destined for pairwise F-H recom-

bination and those that are frozen as correlated pairs. The method using F-aggregate destruction as a probe counts only those H centers which escape pairwise recombination with the complementary F centers and are free to diffuse and finally annihilate an uncorrelated F center or F_2 center.[17,43]

Given this fundamental difference in the two measurements, it is remarkable that the dashed line fits in Fig. 11 as an extension of the best-fit line through our high-temperature data. Sonder found an activation energy of 75 meV for uncorrelated F-H pair production over the temperature range 125–250 K. The uncorrelated pair yield changed by a factor of 20 in this range, in contrast to less than a factor-of-2 change in the total (short-pulse) yield. Yet both methods agree closely at 250 K. If an Arrhenius fit is forced on the short-pulse data above 250 K [Fig. 11(a)], the resulting activation energy is 75 ± 25 meV, in agreement with Sonder's data.

Sonder proposed that the thermal activation of uncorrelated defect production could be explained if most of the F-H pairs are initially produced close enough to attract each other and hence not be observed in an experiment which counts only freely diffusing atoms. The activation energy was proposed to be the difference in barrier heights for jumps carrying the F-H pair to larger or smaller separations.[44]

It is suggested that a similar mechanism may determine the temperature-dependent formation of F centers observable 46 psec after excitation in KCl.[37] We may suppose that the absorption bands of the nearest-neighbor (nn) F-H pair or some other metastable close-pair configuration will be shifted substantially relative to the normal F band. This is observed in fluorite crystals, for example.[45] Since our probe wavelength falls at the peak of the F band, it would be most sensitive to those F-H pairs which achieve sufficient separation (e.g., next-nearest neighbor) to exhibit an absorption band corresponding more nearly to the normal F spectrum. The unstable nearest-neighbor F-H pair could be populated with almost unit efficiency, but our 46-psec measurement might detect only those pairs which achieve thermally activated separation beyond a critical distance. If the thermal energy is supplied from the lattice in equilibrium at a given temperature, the diffusion continues indefinitely and the defects are counted in aggregate-destruction experiments.[17,43] Even if the lattice temperature is too low to support extended diffusion, there is a local thermal spike associated with the rapid liberation of about 1 eV as the system relaxes from the precursor P near $\Sigma_g^+(\sigma_u, \sigma_u)$ to a nearest-neighbor F-H pair. This would allow short-range separation of the vacancy and interstitial, giving the temperature-independent plateau in Fig. 11, as measured shortly after excitation. However because of the limited range of the thermal spike, these defects ultimately recombine in a correlated manner, possibly initiated by electron tunneling, giving a very low yield of defects as measured in Ref. 17. At the upper end of the plateau region (~200 K) the lattice temperature begins to support extended diffusion of a small fraction of the defects beyond the range of the thermal spike. These are observed as uncorrelated defects (dashed line), and finally outnumber the correlated pairs as the total yield rises steeply at high temperature. The model suggested here predicts that most of the vacancies and interstitials will recombine as uncorrelated pairs at high temperature.

The phenomenon we refer to here as a thermal spike may be more accurately described as a special case of the recombination-enhanced defect reaction theory discussed by Kimerling and coworkers,[46] based on the Rice-Ramsperger-Kassel (RRK) theory[47] of unimolecular reactions. The theory addresses the statistical partition of an impulse of vibrational energy (resulting from a nonradiative recombination event) among communicating localized vibrational modes of the "defect molecule," i.e., the point defect and its immediate neighborhood in the lattice. It is assumed that there is a particular vibrational mode which, given sufficient energy, will lead to the defect reaction, e.g., impurity diffusion in semiconductors. The localized vibrational modes decay to lattice phonons, limiting the time in which the recombination-enhanced reaction may occur. This time is typically so short (a few picoseconds or less) that the concept of a thermal spike of molecular dimensions with a characteristic temperature may not be well defined, whereas the RRK statistical theory should be generally applicable. The recombination energy (or some fraction) appears in the theory as an effective reduction of the reaction barrier rather than a rise in local temperature.[46] The typical Arrhenius plot of such a process appears as the sum of the pure thermal process, dominant at high temperature, and the recombination-enhanced process, which may be nearly independent of temperature. The resemblance to our Fig. 11 is striking.

Kimerling has discussed some aspects of F-center production in the context of recombination-enhanced defect reactions.[46] We suggest that the unstable nearest-neighbor F-H pair immediately after formation may be the "defect molecule" in

the terminology of Ref. 46, and that the nonradiative recombination event is the excitonic relaxation leading to that state. The process which is enhanced is H-center motion away from the F center. In contrast to the process of enhanced diffusion in semiconductors,[46] there can be only one such recombination enhancement of H-center motion per F-H pair produced. Thus the recombination-enhanced H-center motion is limited in range, whereas the pure thermal motion may continue indefinitely, producing uncorrelated F-H pairs. This is one explanation for the difference in our observation and Sonder's data (Fig. 11) as discussed above. Note that a single recombination-enhancement step may in principle cause motion over several lattice spacings, so that directional H-center collision sequences are not excluded.

At the lowest temperatures (2–8 K) in Fig. 11(b), the defect yield measured by Karasawa and Hirai indicates a 2-meV barrier. This barrier must occur fairly early in the defect formation process. As discussed above, at least 1 eV is dissipated rapidly in the passage from P to $F+H_{nn}$. It is unlikely that a 2-meV barrier would be significant during or shortly after such a process. Therefore it is reasonable to suppose that the 2-meV barrier governs entry from the precursor STE state (P) to the defect formation channel (Fig. 10).

In Fig. 10, $\Sigma_g^+(\sigma_u, \sigma_u)$ is represented as the STE state from which defect formation is initiated. A calculation by Itoh, Stoneham, and Harker indicates that a barrier of at least 0.3 eV resists translation of a developing H center along a $\langle 110 \rangle$ direction in this state because of a repulsive interaction with the nearest-neighbor alkali ions.[41] However it has been suggested that the alkali-ion repulsion is significantly reduced if the initial motion of the halide-ion pair is rotation out of the $\langle 110 \rangle$ direction.[37] This possibility is indicated by the broken line to the right of P in Fig. 10, and could correspond to the observed 2-meV barrier. Itoh and Saidoh suggested $\Pi_g(\pi_g, \sigma_g)$ as an alternative precursor to defect formation.[34] In that case the right-hand side of Fig. 10 should be altered to connect appropriately to the self-trapping diagram at roughly the Q_1 coordinate marked B.

The temperature dependence exhibited in Fig. 11 might also be ascribed to two different precursor states feeding independent channels of defect production characterized by activation energies of 2 and 75 meV. It would be supposed that at most 20% of the electron-hole pairs feed the 2-meV channel, so that it saturates at a low temperature.

The observed high yield of primary F centers in KCl at high temperature is itself rather remarkable, though not entirely without precedent. Hobbs has observed the formation of sodium colloids due to F-center coalescence in heavily irradiated NaCl at temperatures in the range of 425 K.[48] Jain and Lidiard found that for the best fit of their theory to the experimental data on colloid formation, it was necessary to assume that one primary F-H pair is produced for every 15 eV absorbed.[49] This corresponds to roughly one F-H pair per ionizing event at 425 K, which is comparable to our direct observation of about 0.4 F-H pair per ionizing event in KCl at 450 K. Generalizing from these high-temperature observations and from the trends evident in F-aggregate destruction data for KCl, KI, NaCl, RbCl, and KBr at temperatures below about 250 K,[17,43] it is possible that the yield of primary F-H pairs per ionizing event approaches the order of unity at high temperature in almost all alkali halides.

The approach to unity in Fig. 11 is faster than a simple Arrhenius process would predict. In fact one can make an approximate linear extrapolation of Fig. 8 to unity yield at the melting point of KCl. Ionic conductivity in halide crystals is observed to increase more rapidly than is consistent with a simple Arrhenius process as the melting point is approached.[50] This conductivity anomaly in silver halides has been analyzed in terms of a decreasing Frenkel pair formation energy at increasing temperature.[51]

ACKNOWLEDGMENTS

We wish to thank M. N. Kabler for many helpful discussions, and P. H. Klein for furnishing high-purity KCl samples. We also wish to thank C. H. Leung and K. S. Song, L. C. Kimmerling, C. D. Clark, and J. M. Ortega for helpful comments and for conveying results of their work prior to publication.

APPENDIX: MODELS FOR THE CONVOLUTION OF PULSE SHAPES AND INTRINSIC PHOTOCHEMICAL RESPONSE

Equation (2) in the text displays the basic form of the convolution integrals used in our analysis of data for the rise of optical absorption on a time scale comparable to the laser-pulse duration. Because of the relatively slow response of the photodetector on a picosecond time scale, the experimental quantities G_i in Eq. (1) are effectively time integrals of the probe light intensity. Thus the observed optical density D in Eq. (1) is not the same as the instantaneous optical density $D'(t)$, defined as the base 10 logarithm of reciprocal transmittance at time t. The time-integrated pulses in Eq. (1) can be normalized such that

$$\frac{G_2}{G_1} = \int_{-\infty}^{\infty} dt\, G(t) = 1 \tag{A1}$$

and

$$\frac{G_2'}{G_1'} = \int_{-\infty}^{\infty} dt\, G(t) 10^{-D'(t)} . \tag{A2}$$

The normalized probe pulse envelope is taken to be a Gaussian whose width is the unit of time:

$$G(t) = \pi^{-1/2} e^{-t^2} . \tag{A3}$$

Thus if W_G is the FWHM of $G(t)$, $W_G/2\sqrt{\ln 2} = 1$ by definition in the following discussion and in Fig. 2. The generation of electron-hole pairs (i.e., two-photon excitation) is assumed to be proportional to a normalized Gaussian function $C(t)$ whose center precedes the probe pulse center by a time Δ:

$$C(t+\Delta) = \pi^{-1/2} W^{-1} \exp\left[-\left(\frac{t+\Delta}{W}\right)^2\right]. \tag{A4}$$

Here $W = W_C/W_G$, where W_C is the width of $C(t+\Delta)$. If the time dependence of the onset of $D'(t)$ is expressed as $F(t) = D'(t)/D_{\max}$, substitution of Eqs. (A1) and (A2) into Eq. (1) in the text yields Eq. (2). Here $D_{\max} = a/2.303$ is the maximum value of $D'(t)$, taken to be equivalent to the maximum value of the observed optical density at times much longer than the laser pulse width if the growth is a simple monotonic function. For more complicated growth and decay behavior as in Eqs. (5) and (6), $D_{\max}$ (or C_i) must be regarded as a fitting parameter.

The most general convolution problem of this sort would include cases in which the material system supports a cooperative interaction of the excitation and probe beams. Either these must cooperatively produce an excitation in the sample, or they must participate in generation of a sum or difference frequency. The former requires a real final state in the material and the latter (a three-wave mixing process) requires a noncentrosymmetric material; our materials satisfy neither of these conditions. In contrast, an experiment in which the pump beam produces a real excitation and the probe beam has the same frequency may exhibit interference effects.[52]

We consider now kinetic models for the development of the physical process leading to absorption. If the optical absorption appears instantaneously upon electron-hole generation, substitution of Eq. (A4) in Eq. (3) yields

$$F(t,\Delta)_{\text{instant}} = \tfrac{1}{2}\left[1 + \operatorname{erf}\left(\frac{t+\Delta}{W}\right)\right], \tag{A5}$$

where

$$\operatorname{erf}(x) = 2\pi^{-1/2} \int_0^x e^{-u^2} du .$$

Using Eq. (A5) with a close analytic approximation for erf, it is straightforward to integrate Eq. (2) numerically, obtaining curves such as those in Fig. 2.

For a single probabilistic decay between two levels, characterized by rate γ, the lower-level population is proportional to

$$K(t-t') = 1 - \exp[-\gamma(t-t')] . \tag{A6}$$

Here t' is the time at which the upper level is populated and t is the time at which the lower level is instantaneously interrogated. Taking Eqs. (A4) and (A6) in Eq. (3) and completing the square in the argument of exp yields

$$F(t+\Delta)_e = \tfrac{1}{2}\left[1 + \operatorname{erf}\left(\frac{t+\Delta}{W}\right)\right] - \tfrac{1}{2}\exp\left[-\gamma t + \left(\frac{\gamma W}{2}\right)^2 - \gamma\Delta\right]\left[1 + \operatorname{erf}\left(\frac{t+\Delta}{W} - \frac{\gamma W}{2}\right)\right] . \tag{A7}$$

Equation (A6) pertains to a single probabilistic decay between two levels. The method of Laplace transforms allows treatment of more general problems such as serial decay through n intervals among $n+1$ levels. For example a three-level system in which population of the middle level is observed represents the simplest case of formation and decay of an absorbing species. Serial decay through n intervals prior to population of the observed lowest level gives rise to delayed formation approaching a step function as n becomes large. For "level," one may substitute "photochemical intermediate."

Consider the case of serial decay connecting three levels, where distinct rate constants γ_1 and γ_2 characterize decay from first to second and second to third levels, respectively. If the first level is populated instantaneously at time t', the population of the second level is proportional to

$$[\gamma_1/(\gamma_2 - \gamma_1)](e^{-\gamma_1(t-t')} - e^{-\gamma_2(t-t')}) . \tag{A8}$$

This is equivalent to Eq. (5) in the text, where $\tau_1 = \gamma_1^{-1}$ and $\tau_2 = \gamma_2^{-1}$. The population of the third level is proportional to

$$K_3(t) = 1 - \frac{\gamma_1}{\gamma_1 - \gamma_2} e^{-\gamma_2 t} - \frac{\gamma_2}{\gamma_2 - \gamma_1} e^{-\gamma_1 t}, \qquad \text{(A9)}$$

where $t' = 0$ for convenience in Eq. (A10) and the following discussion.

For the case of n serial decays connecting $n+1$ levels via distinct rate constants, the corresponding expression for population of the last level is

$$K_{n+1} = 1 - \sum_{j=1}^{n} R_j e^{-\gamma_j t},$$

where

$$R_j = \prod_{i \neq j} \frac{\gamma_i}{\gamma_i - \gamma_j}. \qquad \text{(A10)}$$

These forms are singular when any two γ's coincide, but they are valid in a limiting sense even then. Eq. (A10), like (A7), allows completion of the square to perform the convolution integral. The Laplace transform method also is applicable to cases in which some or all the γ's are identical.

For the specific case of serial decay among $n+1$ levels, with all intervals sharing a common γ value, K is replaced by

$$1 - P_n(t)\, e^{-\gamma t},$$

where

$$P_n(t) = \sum_{j=0}^{n-1} \frac{1}{j!} (\gamma t)^j. \qquad \text{(A11)}$$

$P_n(t)$ may be recognized as a truncated series for the exponential. For n large, Eq. (A11) approximates a step function of argument $\gamma t - 1$. Identical rate constants γ are not likely to be encountered in a real system. However, the curves obtained in this model have some value in imparting an appreciation for the large number of intervals which must be involved to approach step-function behavior. This model considers only kinetics of independent centers or molecules; it does not encompass autocatalysis.

[1] M. N. Kabler, in *Point Defects in Solids*, edited by J. H. Crawford, Jr. and L. M. Slifkin (Plenum, New York, 1972), Vol. 1, Chap. 6.
[2] M. N. Kabler, Phys. Rev. 136, A1296 (1964).
[3] R. B. Murray and F. J. Keller, Phys. Rev. 137, A942 (1965).
[4] I. L. Kuusmann, P. Kh. Liblik, and Ch. B. Lushchik, JETP Lett. 21, 72 (1975); T. Hayashi, T. Ohata, and S. Koshino, J. Phys. Soc. Jpn. 42, 1647 (1977).
[5] R. T. Williams and M. N. Kabler, Phys. Rev. B 9, 1897 (1974); R. G. Fuller, R. T. Williams, and M. N. Kabler, Phys. Rev. Lett. 25, 446 (1970).
[6] J. Suzuki and M. Hirai, J. Phys. Soc. Jpn. 43, 1679 (1977).
[7] Y. Kondo, M. Hirai, and M. Ueta, J. Phys. Soc. Jpn. 33, 151 (1972).
[8] J. N. Bradford, R. T. Williams, and W. L. Faust, Phys. Rev. Lett. 35, 300 (1975).
[9] J. W. Davisson and P. H. Klein (private communication).
[10] M. N. Kabler and D. A. Patterson, Phys. Rev. Lett. 19, 652 (1967).
[11] A. E. Purdy, R. B. Murray, K. S. Song, and A. M. Stoneham, Phys. Rev. B 15, 2170 (1977).
[12] R. T. Williams, M. N. Kabler, and I. Schneider, J. Phys. C 11, 2009 (1978).
[13] M. Ikezawa and T. Kojima, J. Phys. Soc. Jpn. 27, 1551 (1969).
[14] D. Pooley and W. A. Runciman, J. Phys. C 3, 1915 (1970).
[15] K. Teegarden and G. Baldini, Phys. Rev. 155, 896 (1967).
[16] D. Fröhlich and B. Staginnus, Phys. Rev. Lett. 19, 496 (1967).
[17] E. Sonder, Phys. Rev. B 12, 1516 (1975).
[18] D. Y. Smith and D. L. Dexter, in *Progress in Optics*, edited by E. Wolf (North-Holland, Amsterdam, 1972), Vol. 10, p. 167.
[19] *Landolt-Börnstein Zahlenwerte und Functionen, II Band, 8 Teil* (Springer-Verlag, Berlin, 1962), p. 419.
[20] J. D. Konitzer and J. J. Markham, J. Chem. Phys. 32, 843 (1960).
[21] M. Hirai, Y. Kondo, T. Yoshinari, and M. Ueta, J. Phys. Soc. Jpn. 30, 440 (1971).
[22] A. E. Purdy and R. B. Murray, Solid State Commun. 16, 1293 (1975).
[23] E. Sonder and W. A. Sibley, in *Point Defects in Solids*, edited by J. H. Crawford, Jr. and L. M. Slifkin (Plenum, New York, 1972), Vol. 1, p. 258.
[24] M. Ueta, Y. Kondo, M. Hirai, and T. Yoshinari, J. Phys. Soc. Jpn. 26, 1000 (1969).
[25] See, for example, Can. J. Chem. 55, No. 11 (1977).
[26] C. D. Clark (private communication).
[27] *Color Centers in Solids*, J. H. Schulman and W. D. Compton (Pergamon, New York, 1962), p. 76.
[28] C. D. Clark, A. H. Skull, and J. S. Wells, in International Conference on Defects in Insulating Crystals, Gatlinburg, 1977 (unpublished).
[29] R. T. Williams, P. H. Klein, and C. L. Marquardt, in *Proceedings of the Conference on Laser Induced Damage in Optical Materials: 1977*, U. S. Natl. Bur. Stand. Spec. Pub. No. 509, edited by A. J. Glass and A. H. Guenther (U.S. GPO, Washington, D. C., 1978), p. 481.
[30] I. M. Catalano, A. Cingolani, and A. Minafra, Phys. Rev. B 5, 1629 (1972).
[31] D. H. Auston, C. V. Shank, and P. LeFur, Phys. Rev. Lett. 35, 1022 (1975); J. S. Blakemore, *Semiconductor Statistics* (Pergamon, New York, 1962), p. 214.
[32] D. Pooley, Proc. Phys. Soc. 87, 245 (1966).
[33] M. N. Kabler, in *Proceedings of the NATO Advanced Study Institute on Radiation Damage Processes in Materials, Corsica, 1973*, edited by C. H. S. Dupuy (Noordhoff, Leyden, 1975), p. 171.
[34] N. Itoh and M. Saidoh, J. Phys. Colloq. 34, C9-101 (1973).
[35] Y. Toyozawa, in *Proceedings of the Fourth International Conference on Vacuum Ultraviolet Radiation Physics, Hamburg, 1974*, edited by E. E. Koch, R. Haensel, and C. Kunz (Pergamon, Vieweg, 1974),

p. 317.
[36]Y. Toyazawa, J. Phys. Soc. Jpn. 44, 482 (1978).
[37]M. N. Kabler and R. T. Williams, Phys. Rev. B 18, 1948 (1978).
[38]R. Smoluchowski, O. W. Lazareth, R. D. Hatcher, and G. J. Dienes, Phys. Rev. Lett. 27, 1288 (1971).
[39]M. Saidoh and N. Itoh, Phys. Status Solidi B 72, 709 (1975).
[40]C. H. Leung and K. S. Song, Phys. Rev. B 18, 922 (1978).
[41]N. Itoh, A. M. Stoneham, and A. H. Harker, J. Phys. C 10, 4197 (1977).
[42]T. Karawawa and M. Hirai, J. Phys. Soc. Jpn. 40, 769 (1976).
[43]G. Guillot, A. Nouailhat, and P. Pinard, J. Phys. Soc. Jpn. 39, 398 (1975).
[44]E. Sonder, J. Phys. Colloq. 34, C9-483 (1973).
[45]R. T. Williams, M. N. Kabler, W. Hayes, and J. P. Stott, Phys. Rev. B 14, 725 (1976).
[46]L. C. Kimerling, in Conference on Recombination in Semiconductors, Southampton, 1978 (unpublished); J. D. Weeks, J. C. Tully, and L. C. Kimerling, Phys. Rev. B 12, 3286 (1975).
[47]K. J. Laidler, *Theories of Chemical Reaction Rates* (McGraw-Hill, New York, 1969).
[48]L. W. Hobbs, *Surface and Defect Properties of Solids*, Vol. 4 (The Chemical Society, London, 1975), p. 152.
[49]U. Jain and A. B. Lidiard, Philos. Mag. 35, 245 (1977).
[50]L. M. Slifkin, in International Conference on Defects in Ionic Crystals, Gatlinburg, 1977 (unpublished).
[51]J. Aboagye and R. Friauf, Phys. Rev. B 11, 1654 (1975).
[52]E. P. Ippen and C. V. Shank, in *Ultrashort Light Pulses*, edited by S. L. Shapiro (Springer-Verlag, Berlin, 1977), p. 110.